

Supplemental information

**lncRNA MIR210HG promotes the progression
of endometrial cancer by sponging miR-337-3p/137
via the HMGA2-TGF- β /Wnt pathway**

Jian Ma, Fan-Fei Kong, Di Yang, Hui Yang, Cuicui Wang, Rong Cong, and Xiao-Xin Ma

Supplementary Table S1

Table S1: qRT-PCR was used to detected the expression of MIR210HG mRNA expression and analyzed the clinicopathologic characteristics of endometrial cancer patients.

Clinical pathological parameters		N = 40	MIR210HG Mean ± SEM	P
Age	< 60	28	4.016 ± 1.031	0.7771
	≥ 60	12	3.448 ± 1.872	
Clinical stage	I + II	28	1.607 ± 0.282	0.0001
	III + IV	12	9.068 ± 2.371	
Differentiation	High	16	2.049 ± 0.432	
	Middle	14	5.032 ± 1.839	0.1043
	Low	10	5.059 ± 2.411	0.1380
Infiltration degree	< 1/2 Muscle layerer	33	3.502 ± 0.906	0.4151
	≥ 1/2 Muscle layerer	7	5.466 ± 3.007	
Lymphnode metastasis	Negative	33	2.512 ± 0.653	0.0007
	Positive	7	10.13 ± 3.393	
Distal metastasis	Negative	38	3.922 ± 0.949	0.7163
	Positive	2	2.389 ± 0.354	

Note:

P = 0.1043, High differentiation vs. Middle differentiation;

P = 0.1380, High differentiation vs. Low differentiation.

Note:

FIGO stage: I+II *vs.* III+IV;

Differentiation: $P > 0.9999$, High differentiation *vs.* Middle differentiation; $P =$

0.0154, High differentiation *vs.* Low differentiation

Supplementary Table S2

Table S2: *In situ hybridization analysis* was used to detected the expression of MIR210HG in normal endometrial tissue and endometrial carcinoma tissue, and analyzed the relationship between the expression of MIR210HG and clinicopathological parameters.

Clinical pathological parameters	N	MIR210HG		<i>P</i>
		(-)	(+)	
Age				0.0292
< 60	54	14	40	
≥ 60	24	1	23	
FIGO stage				0.0439
I	17	5	12	
II	16	5	11	
III	34	4	30	
IV	11	1	10	
Differentiation				
High	27	7	20	
Middle	31	8	23	>0.9999
Low	20	0	20	0.0154
Muscular invasion				0.0010
< 1/2	43	14	29	
≥ 1/2	35	1	34	
Lymphnode metastasis				0.0700
Negative	50	13	37	
Positive	28	2	26	

Note:

FIGO stage: I+II vs. III+IV;

Differentiation: $P > 0.9999$, High differentiation vs. Middle differentiation; $P = 0.0154$, High differentiation vs. Low differentiation

Supplementary Table S3

Table S3: Association between miR-337-3p mRNA expression and endometrial cancer patients clinicopathologic characteristics

Clinical pathological parameters		N = 40	miR-337-3p Mean ± SEM	P
Age	< 60	28	0.151 ± 0.029	0.7155
	≥ 60	12	0.168 ± 0.033	
Clinical stage	I + II	28	0.207 ± 0.026	0.0002
	III + IV	12	0.037 ± 0.005	
Differentiation	High	16	0.204 ± 0.043	
	Middle	14	0.116 ± 0.030	0.1104
	Low	10	0.136 ± 0.035	0.2713
Infiltration degree	< 1/2 Muscle layerer	33	0.167 ± 0.025	0.3023
	≥ 1/2 Muscle layerer	7	0.106 ± 0.040	
Lymphnode metastasis	Negative	33	0.180 ± 0.025	0.0145
	Positive	7	0.041 ± 0.008	
Distal metastasis	Negative	38	0.163 ± 0.023	0.1695
	Positive	2	0.023 ± 0.001	

Note:

 $P = 0.1104$, High differentiation vs. Middle differentiation; $P = 0.2713$, High differentiation vs. Low differentiation.

Supplementary Table S4

Table S4: Association between miR-137 mRNA expression and endometrial cancer patients clinicopathologic characteristics

Clinical pathological parameters		N = 40	miR-137 Mean ± SEM	P
Age	< 60	28	0.044 ± 0.008	0.3238
	≥ 60	12	0.064 ± 0.025	
Clinical stage	I + II	28	0.066 ± 0.012	0.0060
	III + IV	12	0.013 ± 0.003	
Differentiation	High	16	0.070 ± 0.020	
	Middle	14	0.036 ± 0.008	0.1500
	Low	10	0.038 ± 0.009	0.8575
Infiltration degree	< 1/2 Muscle layerer	33	0.051 ± 0.011	0.7325
	≥ 1/2 Muscle layerer	7	0.043 ± 0.014	
Lymphnode metastasis	Negative	33	0.058 ± 0.011	0.0513
	Positive	7	0.011 ± 0.005	
Distal metastasis	Negative	38	0.051 ± 0.009	0.5654
	Positive	2	0.027 ± 0.004	

Note:

P = 0.1500, High differentiation vs. Middle differentiation;

P = 0.8575, High differentiation vs. Low differentiation.

Supplementary Table S5

Table S5: The sh-RNA cloned and agomir and antagonir sequences.

Name	Sequence
LV3-MIR210HG –	5’-
RNAI-1	CCCACUUGGCCUAUGCAUUTT-3’
LV3-MIR210HG –	5’-
RNAI-2	GAAAUAACCAAGCCGAGUUTT -3’
LV3-MIR210HG –	5’-
RNAI-3	CCAUGGAACACAGCUUUGAAUTT-3’
LV3-NC	5’-
	TTCTCCGAACGTGTACGT-3’
miR-NC	Sense: 5’-UUCUCCGAACGUGUCACGUTT-3’ Antisense: 5’-ACGUGACACGUUCGGAGAATT-3’
Agomir-337-3p	Sense: 5’-CUCCUUAUGAUGCCTUUUCUUC -3’ Antisense: 5’-AGAAAGGCAUCAUAUAGGAGUU -3’
Antagomir-337-3p	Sense: 5’-GAAGAAAGGCAUVAUUAUAGGAG -3’
Agomir-137	Sense: 5’-UUAUUGCNUAAGAAUACCGGUAG-3’ Antisense: 5’-AAUAACGAAUUCUUAUGCGCAUC-3’ Sense: 5’-UCACCAUUGCNUAAGUGCAAUU-3’
Antagomir-137	5’-
HMGA2-RNAi (4487-1)-a	GATCCCCAAGAGGCAGACCTAGGAAACTCGAG TTTCCTAGGTCTGCCTCTGGTTTGAT-3’
HMGA2-RNAi (4487-1)-b	5’- AGCTATCCAAAAACCAAGAGGCAGACCTAGGAAA CTCGAGTTCCCTAGGTCTGCCTCTGGGG-3’

Supplementary Table S6

Table S6: Primer sequences for qRT-PCR and *in situ hybridization*.

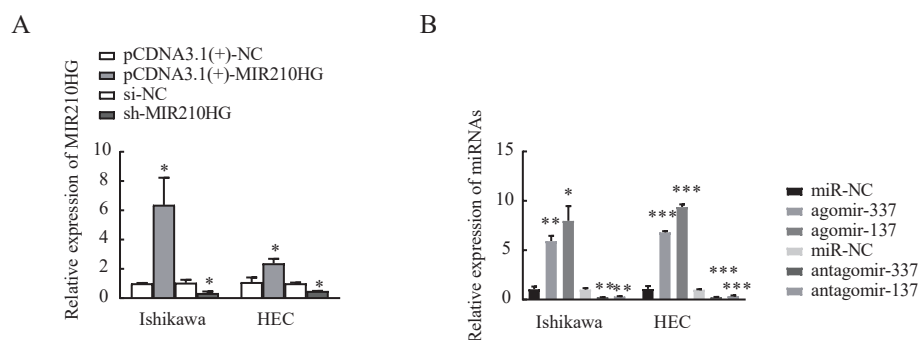
Name	Sequence
MIR210HG	F: GCAGGCACAGGTGTGGTCATATC R: AGGCAGGCTCAGCAGACAGG
has-miR-337-3p	F: CTCCTATATGATGCCTTCTTC
has-miR-137	F: TTATTGCTTAAGAATAACGCGTAG
GAPDH	F: GCACCGTCAAGGCTGAGAAC R: TGGTGAAGACGCCAGTGGA
U6	F: CGGGTTTGTTCGCATTCT R: AGTCCCAGCATGAACAGCTT
MIR210HG probe-1	5' – AGCTA GGCAT GGTGG TGGC ACCTG TAATC CCAGC TACTT – 3'
MIR210HG probe-2	5' – CACTT GGCCT ATGCA TTCCA GGCTC CATCC CATGT GACTC – 3'
MIR210HG probe-3	5' – AGCCT CCTGC TGCTG CCTGG CTTCC CTGCA TTCCC TGTTC – 3'
HMGA1P1	F: ACGGCTCCAAGAAGGCTCTCC R: GCTCCGCTTCTCAGTGCCATC
HMGA2	F: CTCAAAAGAAAGCAGAAGCCACTG R: TGAGCAGGCTTCTTCTGAACAACT

Supplementary Table S7

Table S7: Primary antibodies used for the detection of protein expression

Name	Manufacturer	Dilution ratio: Western blotting, Immunohistochemistry
HMGA2	Abcam, Cambridge, UK	1:1000, 1:400
E-cadherin	Cell Signaling Technology, Inc., Danvers	1:1000
TGF-β RII	Abcam, Cambridge, UK	1:1000
β-catenin	Cell Signaling Technology, Inc., Danvers	1:500
SMAD3	Abcam, Cambridge, UK	1:1000
p-SMAD3	Abcam, Cambridge, UK	1:500
Snail	Proteintech, Hangzhou, China	1:200
Ki-67	Santa Cruz, CA	1:200, 1:400
Ago2	Abcam, Cambridge, UK	1:200
GAPDH	Proteintech, Hangzhou, China	1:5000
p-GSK-3β	Abcam, Cambridge, UK	1:1000
c-myc	Proteintech, Hangzhou, China	1:500

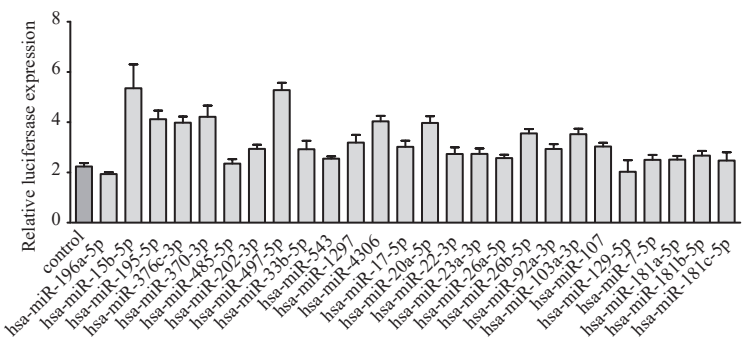
Supplementary Figure S1



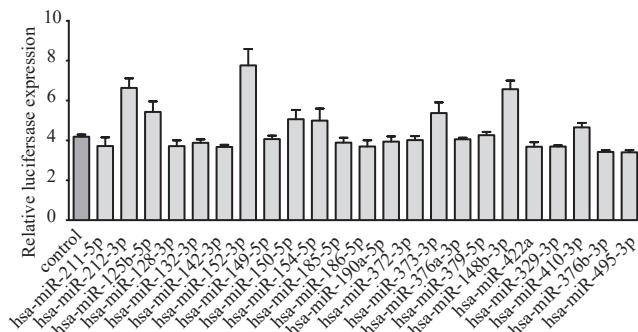
(A) qRT-PCR was used to determine the transfection efficiency of MIR210HG. (B) qRT-PCR was used to determine the transfection efficiency of the miRNAs. Data are presented as the mean \pm SEM ($n = 3$ per group). * $P < 0.05$, ** $P < 0.01$, *** $P < 0.001$.

Supplementary Figure S2

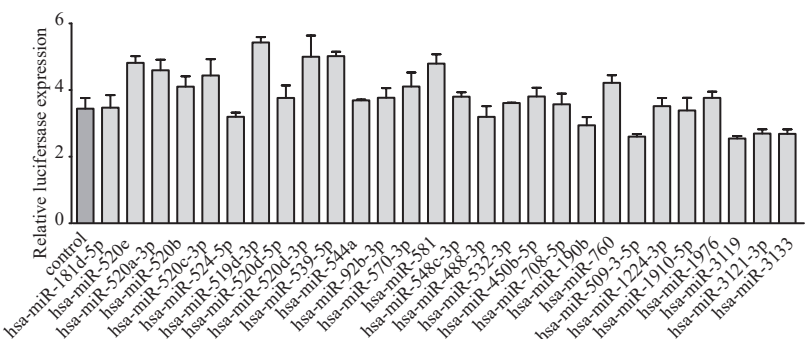
A



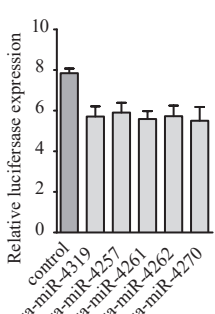
B



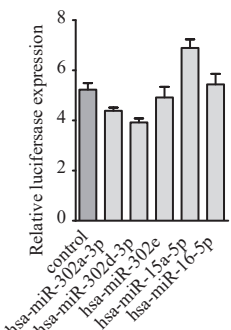
C



D



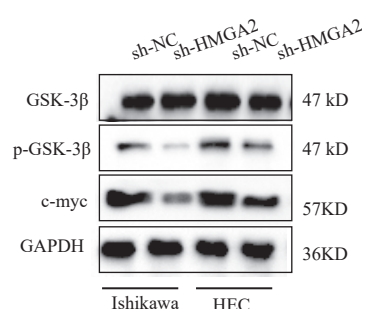
E



(A) and (E). Luciferase reporter assay using HEK293T cells co-transfected with HMGA2-WT and the indicated miRNA. Data are presented as the mean \pm SEM ($n = 3$ per group). * $P < 0.05$, ** $P < 0.01$, *** $P < 0.001$.

Supplementary Figure S3

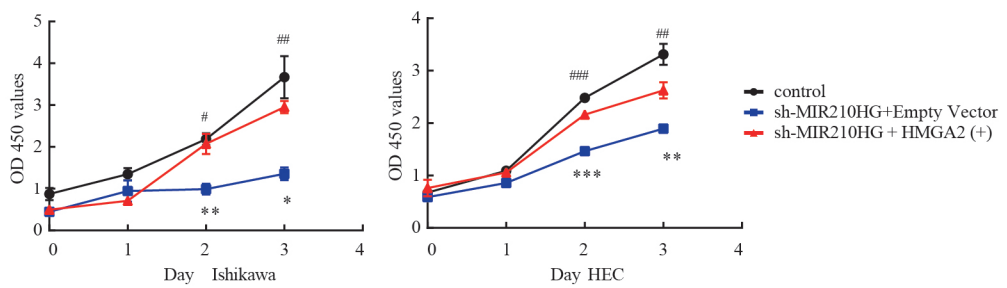
A



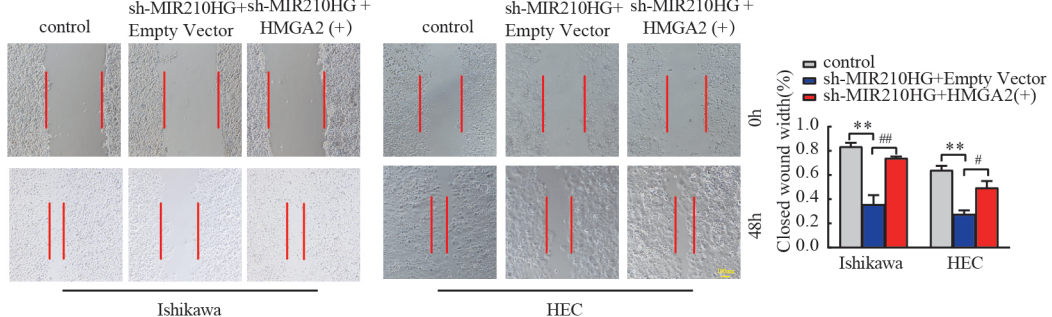
(A) Western blot analysis of the expression of GSK-3 β , p-GSK-3 β ^{ser-9}, and c-myc proteins in response to HMGA2 in Ishikawa and HEC-1A cell lines.

Supplementary Figure S4

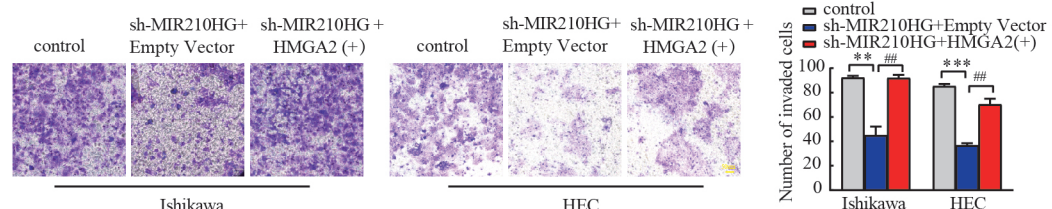
A



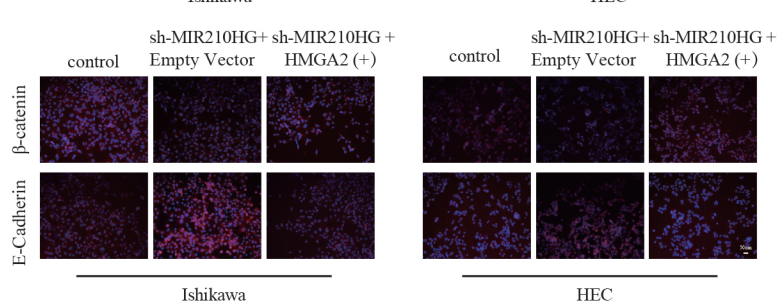
B



C



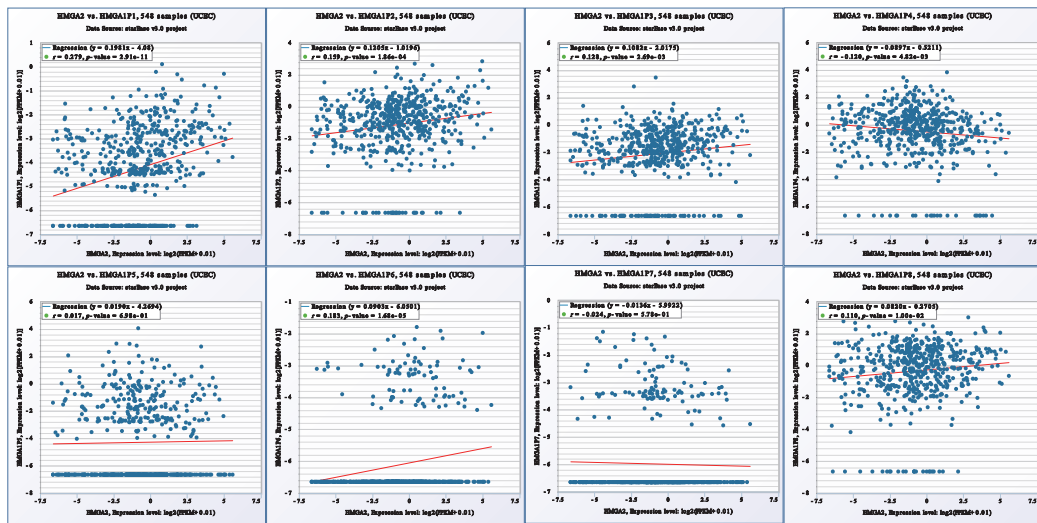
D



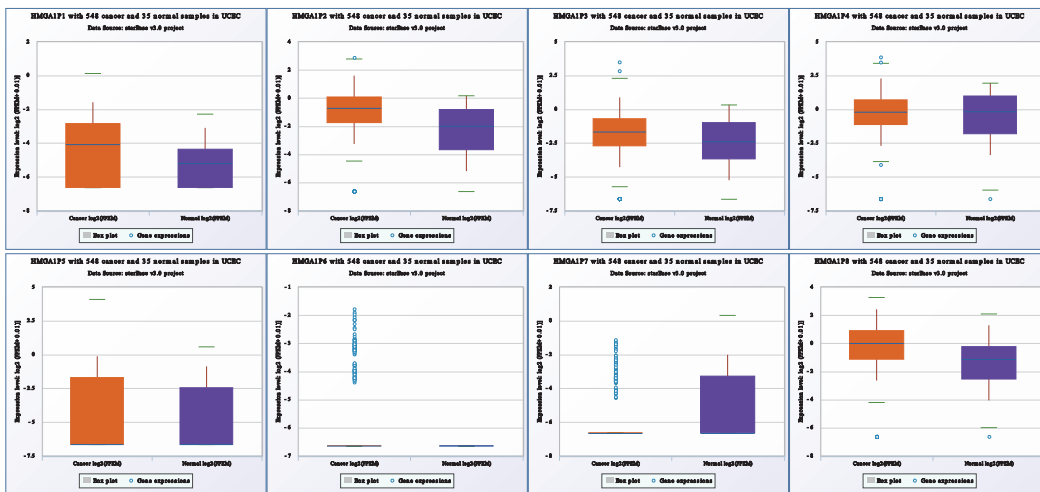
(A) CCK-8 assays to evaluate proliferation in Ishikawa and HEC-1A cell lines. (B) Wound healing assays to investigate the migratory ability of the cells. (C) Transwell assays to determine quantities of invading cells. (D) β -catenin and E-cadherin were analyzed using immunofluorescence staining in Ishikawa and HEC-1A, respectively. Representative images and statistical plots are presented. Data are presented as the mean \pm SEM, ($n = 3$). *P < 0.05, **P < 0.01, ***P < 0.001 vs. control, #P < 0.05, ##P < 0.01, ###P < 0.001 vs. sh-MIR210HG.

Supplementary Figure S5

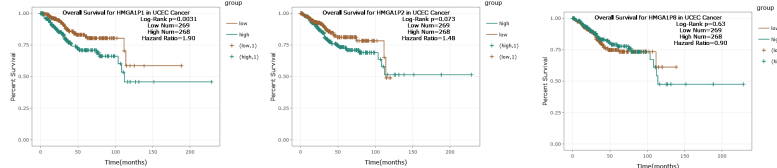
A



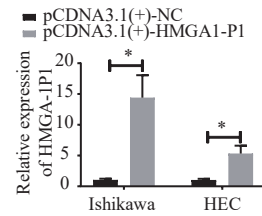
B



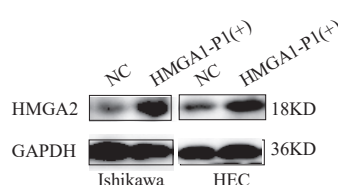
C



D



E



(A) Correlation between the levels of HMGAl-P2 and HMGAl-P3 in endometrial cancer (TCGA cohort).

(B) HMGAl-P2 mRNA expression in endometrial cancer and normal tissue (TCGA cohort).

(C) Kaplan-Meier survival curve for HMGAl-P1, HMGAl-P2, HMGAl-P3 in endometrial cancer (TCGA cohort).

(D) qRT-PCR was used to determine the transfection efficiency of HMGAl-P1. Data are presented as the mean \pm SEM (n = 3 per group). *P < 0.05, ** P < 0.01, *** P < 0.001.

(E) Western blotting assay was performed to analyze the expression of HMGAl-P1.